Third International Workshop on Advanced Computational Intelligence
August 25-27, 2010 - Suzhou, Jiangsu, China

Segmentation of Blood Vessels in Fundus Color Images by Radon Transform and Morphological Reconstruction

Reza Pourreza, Hamidreza Pourreza, Touka Banaee

***Abstract*— In this paper we have presented an algorithm for vessel detection in retinal color images which works based on local Radon transform and morphological reconstruction. In our previous work, the algorithm was applied to conjunctival images and the performance was evaluated subjectively. In this work an extended version of the algorithm is applied to retinal images and our aim is to detect vessels in retinal images of patient people and make a good discrimination between blood vessels and other pathological elements like microaneurysms and hemorrhages which have the same color as vessels. The algorithm performance was evaluated numerically by applying it to DRIVE image database and the achieved ROC curve demonstrates its high accuracy.**

I. Introduction

EYE is the only organ in the living subject where small vessels are directly visible, either in conjunctiva or in retina. Diabetic retinopathy is a well-known microvascular complication of diabetes [1]. The quantification of vessel features such as length, width, tortuosity and branching pattern, among others, can provide new insights to diagnose and stage pathologies which affect the morphological and functional characteristics of blood vessels. However, when the vascular network is complex or the number of images is large, manual measurements can become tiresome or even impossible. Besides clinical analysis is an observer-dependent task which may not be reproducible. A feasible solution is the use of automated analysis which is nowadays commonly accepted by medical community [2].

The mentioned features of blood vessels have diagnostic relevance and can be used to monitor the progression of diseases. Moreover blood vessels, being invariant features, may be very useful for registration of retinal images the same patient gathered from different sources [3]. However, other pathological elements like microaneurysms (MAs) or hemorrhages (HEs) highly affect the accuracy of automated vessel detection system, because they appear in retina with same color of vessels and also HEs have no distinct shape and it is too likely to detect them as vessels. In addition other causes like the presence of noise, low contrast between vasculature and background, variability of vessels width, brightness and shape, make accurate vessel segmentation is a difficult task.

Manuscript received March 31, 2010.

Reza Pourreza is pursuing his PhD program in computer engineering department, Ferdowsi University of Mashhad, Iran (phone: +98-915-3257806; e-mail: pourreza.reza@yahoo.com).

Hamidreza Pourreza is an associate professor in computer engineering department, Ferdowsi University of Mashhad, Iran (e-mail: hpourreza@um.ac.ir).

Touka Banaee is an assistant professor in Ophthalmic Research Center, Khatam-Al-Anbia Hospital, Medical Sciences University of Mashhad, Iran (e-mail: banaeet@mums.ac.ir).

Several methods have been proposed in the literature to address these problems including matched filtering [4], tracking methods [5-7], multi-threshold probing [8], mathematical morphology [9], or a combination of non-linear filtering and morphological operations [2].

The lack of a robust algorithm encouraged us in this work to develop an algorithm for segmentation of blood vessels in fundus color images which is robust against the appearance of MAs, HEs and exudates (EXs) in retina.

The rest of paper is organized in three sections. Section 2 is dedicated to explain the algorithm steps in details. Achieved results are discussed in section 3 and in the last section we conclude our work.

II. Proposed Algorithm

The proposed algorithm consists of six main steps which are depicted in fig. 1.

In the preprocessing step, our aim is to unify the histogram of all available images. In exudates detection step, those regions of image that EXs appear are detected and removed. In background elimination the image background is filtered to some extent and the foreground remains for further processing. All red parts of retina including MAs, HEs and vessels are extracted in mask creation step. The regions of image that are likely to contain thick vessels are detected in marker creation and eventually blood vessels are discriminated from HEs and MAs in the last step using morphological reconstruction. The main six steps of our algorithm are investigated in the following six subsections.

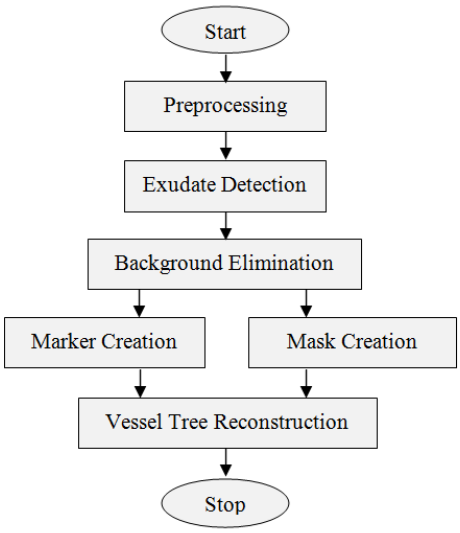

Fig. 1. Vessel segmentation procedure

978-1-4244-6337-4/10/$26.00 @2010 IEEE

A. Preprocessing

By performing preprocessing, we provide an image with maximum possible vessel/background contrast and also unify the histogram of the available images. The fundus images are colored and have three components (R, G, B); however, since the green channel exhibits the best vessel/background contrast, it is selected as input image (I).

We unify the histogram of images because in the following step of algorithm a threshold is used for binarization. Since different images have different brightness and contrast, this is performed to enable us to use the same threshold for all images. For this purpose a reference image is selected and the threshold is adjusted. To unify the images, histogram specification is used and the histogram of I is changed to be like the histogram of green channel of reference image.

B. Exudates Detection

Exudates appear in G component of fundus image as bright regions. Image binarization is chosen to detect EXs, so a mask containing all exudates is created (ex_mask). Despite, in addition to EXs, there are some other bright areas in I such as Optic Nerve Head (ONH). Although we remove the EXs from I, detection of bright parts of ONH instead of EXs has no negative effect vessel segmentation accuracy.

The detected EXs should be removes because they make severe problems in background elimination step. Hence the grey levels of those pixels of I which their corresponding pixels in ex_mask are white are replaced by the mean of I. This is shown (1).

$$I \leftarrow I \times (1 - ex\_mask) + mean(I) \times ex\_mask \quad (1)$$

Fig. 2 shows a sample result of this operation.

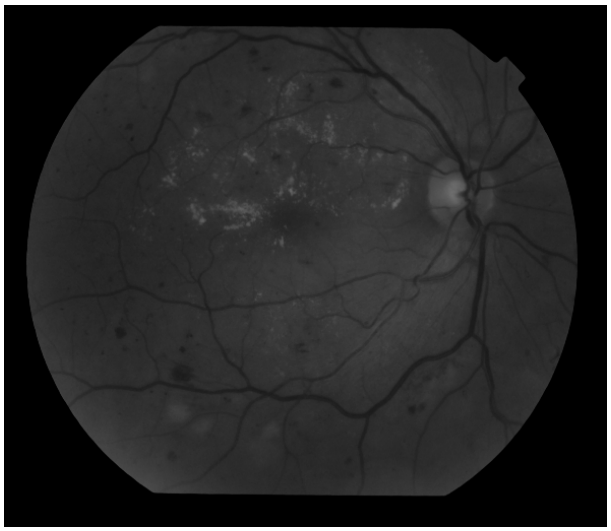

(a)

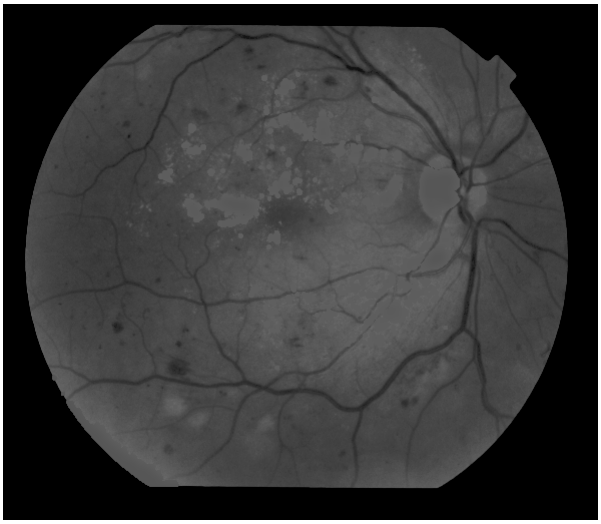

(b)

Fig. 2. The result of exudates detection, a) input image, b) EXs detection result (after histogram specification)

C. Background Elimination

In the fundus images, the background brightness is not the same in the whole image. This varying background would lead to missed vessels or false vessel detection in the following steps. Moreover, in I, background is brighter than the details, but we prefer that the vessels and other components appear brighter than background. These two problems addressed in this step. To overcome the second problem, I in inverted as shown in (2).

$$I \leftarrow 255 - I \quad (2)$$

Since we need a uniform background, its effect should be removed as much as possible. For this purpose, the image is firstly filtered using as average filter with a big window. The result of this filtering would exhibit the background well. Hence if the filtered image is subtracted from the main one, the background would be eliminated to some extent. This operation is formulated in (3).

$$I \leftarrow I - avg\_filter(I) \quad (3)$$

The result of background elimination is shown in fig. 3.

D. Mask Creation

The input is preprocessed up to this step and is now ready for main processing. As mentioned in "Introduction" section, this algorithm has a conditional reconstruction base, hence we need a mask which contains all red details of image and a marker which is a starting point for reconstruction. Red parts of fundus image including MAs, HEs, and vessels appear as bright regions in I. The brightness is used as the main feature and a local Radon transform-based method is implemented for detection of them. This method is explained in [1]; however it is briefly explained here to make it easy for the reader to pursue the algorithm. Mask creation main steps are depicted in fig. 4.

This method uses a sliding window to localize processing. The sliding window has an overlapping factor which means that the neighbor windows are not separated and are overlapped. Defining the window size (n) and sliding factor ($step$), overlapping is shown in fig. 5.

Radon transform is applied to each window. The aim of applying Radon transform is to detect sub-vessels in local windows; however, HEs and MAs are detected. Before applying Radon transform, local window is masked using a circular mask to eliminate the diagonal effect of this transform. Since Radon transform has an integral nature, diagonal angles are more likely to contain the peak of transform, while we expect the peak of transform to occur in a direction that a probably sub-vessel lays. By applying Radon transform that is formulated in (4) in its continuous form, we acquire a matrix (R) that each column is the projection of window in a special angle.

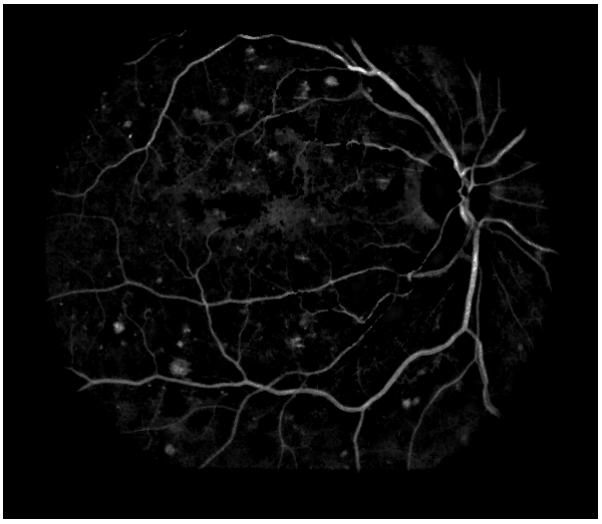

Fig. 3. The result of background elimination

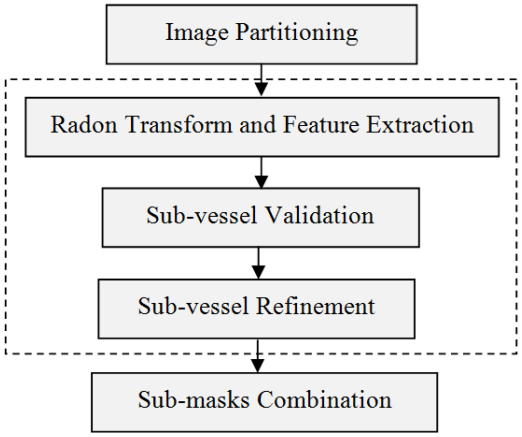

Fig. 4. Mask creation procedure.

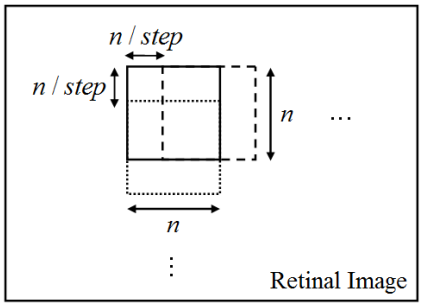

Fig. 5. Overlapping parameters.

$$R(\rho,\theta)=\int_{-\infty}^{+\infty}\int_{-\infty}^{+\infty} g(x,y)\delta(\rho-x\cos\theta-y\sin\theta)dxdy \quad (4)$$

The maximum of R is found and the corresponding projection and angle are kept to extract the sub-vessel information including the angle, start point and end point. If the maximum (m) is greater than a predefined threshold (t_m), the presence of sub-vessel is confirmed. If the presence is confirmed, vessel width is calculated; for this purpose we start in m-containing projection from m index (i_m) and continue to both right and left till we reach $l\times m$. The corresponding indexes that their amplitude in projection are equal or less than $l\times m$ are kept as i_s and i_e since they present line starting and ending points.

Using line angle, i_s, and i_e a white line is drawn in an $n\times n$ black window. The extracted sub-vessel is compared with real one to refine the acquired result. To do this, two thresholds (t_1 and t_2) are extracted from local window and the local window in binarized using the mean of t_1 and t_2. t_1/t_2 is the mean of those pixels of local window that their corresponding pixels in the extracted sub-vessel lay in white/black region. The binarized window is multiplied by the extracted sub-vessel to acquire the refined sub-vessel. Refined sub-vessels extracted from different local windows are then combined considering the overlapping ratio to make the $mask$. Mask already created, that contains MAs, HEs, and vessels, is kept for the last step of algorithm. A sample created mask is shown in fig. 6.

E. Marker Creation

The second essential component for conditional reconstruction is marker. Mask made in previous step contains all red parts, while our desire is blood vessels. Since MAs and HEs are mostly separated from vessels, if marker contains some white pixels on vessel tree, we would be able to reconstruct the whole vessel tree. Marker to be created in this step will be in our desire form and will contain the thick vessels of vessel tree.

MAs are small red spots on the surface of fundus, while HEs are red regions with no distinct shape and are much bigger than MAs. We have used the roundness of bright regions in I as a feature to keep thick vessels and eliminate other bright regions. Hence a sliding window is implemented like "mask creation" step. Radon transform is utilized in each window to extract brightness and non-roundness features. Brightness feature (f_b) is the maximum of R. To extract non-roundness feature (f_r), the maximum-containing column of R is considered as a reference vector. Then the summation of bin-by-bin subtraction of all projections and the reference vector is calculated as (5).

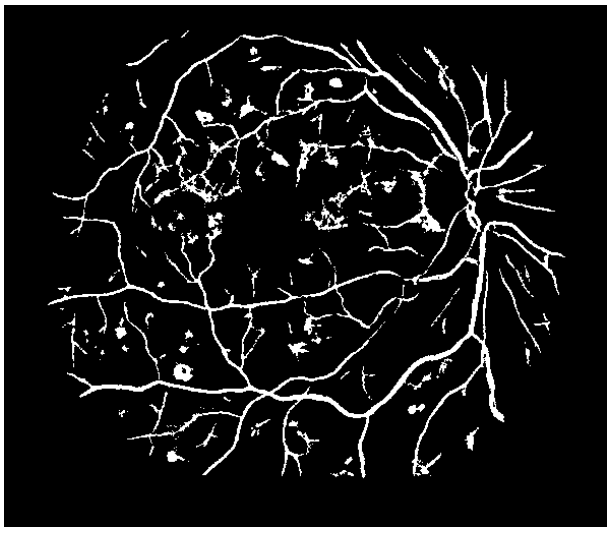

Fig. 6. Sample created mask

$$f_r = \sum_{j=1}^{N}\sum_{k=1}^{M}(R_{jk} - R_{rk})^2 \quad (5)$$

Where R_{jk} is the $(j,k)^{\text{th}}$ component of R matrix, M and N are the dimensions of R ($R_{M\times N}$), and r is the index of reference column in R.

When the sliding window lays in dark regions of I, both f_b and f_r have low values, when it lays on MAs and narrow vessels f_b takes a medium and f_r takes a low value. On HEs, f_b has a high and f_r has a low value and finally on thick vessels, both f_b and f_r take high values. Taking these two features and considering two thresholds, t_b and t_r, the local windows which contain thick vessels are detected. These thick vessels are constructed in a binary image, *marker*, using the vessel refinement procedure explained in previous section. A sample created marker is shown in fig. 7.

F. Vessel Tree Reconstruction

The marker and mask, created in two prior sections, are used to achieve the final vessel map by morphological reconstruction. For this purpose, the conditional dilation operator is utilized which starts from marker image and performs an iterative dilation conditioned to mask. However, because the marker image must be equal or less than mask, marker is first multiplied by mask and then the conditional dilation is performed. Since HEs and MAs are separated from vessels and they do not exist in marker, they do not appear in the final vessel map that is the output of conditional dilation. The final vessel map which is the output of proposed algorithm is shown in fig. 8.

III. Results

The performance of our algorithm is evaluated by applying it to two fundus image databases. The first one is our database which contains the retinal images of the left and right eyes of over 100 people including healthy and different levels patients. Since there is no ground-truth for our database, the results of this database were evaluated subjectively by a physician. To assess the algorithm numerically, we applied it to DRIVE database. Although the images of DRIVE database are mostly taken from healthy people, the results of this database enabled us to compare the performance of our algorithm with some other algorithms.

The dimension of images in our database was 1031×1535, n was set to 27, (n is usually twice bigger than the width of thickest vessel in image), *step* was 3, t_m, t_r, and t_b were set to 4.9, 1.7 and 8 respectively.

The dimension of images in DRIVE database was 512×512, n was set to 13, , *step* was 3, t_m, t_r, and t_b were set to 2.5, 0.65, and 4 respectively.

Comparison of our algorithm performance with other algorithms is performed by drawing its ROC curve beside ROC curve of other algorithms. The two axes in ROC curve are true positive rate (TPR) and false positive rate (FPR). We acquired this curve by varying t_m and it is shown in fig. 9.

The closer the curve to $TPR = 1$ line (similar to step function), the higher accuracy of algorithm. As can be seen in fig. 9, our curve is over five other algorithms in most parts and this fact demonstrates its high accuracy.

Fig. 7. Sample created marker

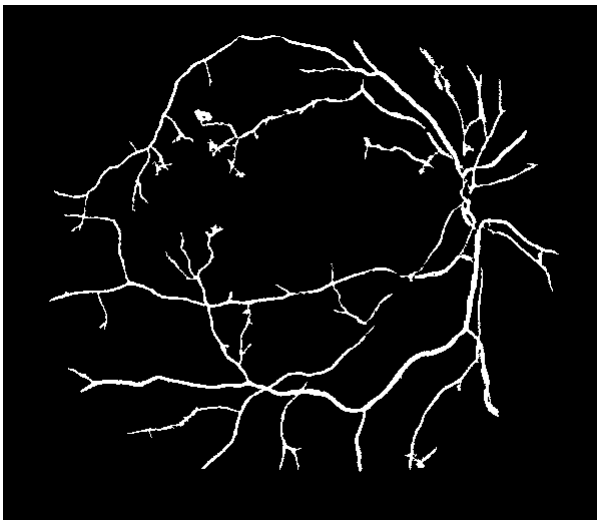

Fig. 8. Final segmented vessel map

IV. Conclusion

In this work we have presented an algorithm for vessel tree extraction in color fundus images. This algorithm is an extension of our previous work which was applied to conjunctival images. The algorithm is able to detect the vessel map in retinal images of patient people which contain pathological elements like MAs and HEs. To discriminate between blood vessels and MAs and HEs, we have used conditional dilation. This morphological operator needs two principal components, mask and marker. These two components are made by using Radon transform as a feature extractor. Our achieved results are comparable with other available approaches and demonstrate the high accuracy in extraction task.

References

[1] R. Pourreza, T. Banaee, H.R. Pourreza, R. Daneshvar, "A Radon transform based approach for extraction of blood vessels in conjunctival images", MICAI 2008, LNAI 5317, pp. 948–956, 2008.

[2] A.M. Mendonça, A. Campilho, "Segmentation of retinal blood vessels by combining the detection of centerlines and

morphological reconstruction", IEEE Transaction on Medical Imaging, Vol. 25, N. 9, pp. 1200-1213, 2006.
[3] E. Ricci, R. Perfetti, "Retinal blood vessel segmentation using line operators and support vector classification", IEEE Transaction on Medical Imaging, Vol. 26, No. 10, pp. 1357-1365, 2007.
[4] S. Chauduri, S. Chatterjee, N. Katz, M. Nelson, M. Goldbaum, "Detection of blood vessels in retinal images using two-dimensional matched filters", IEEE Transaction on Medical Imaging., Vol. 8, No. 3, pp. 263–269, 1989.
[5] I. Liu, Y. Sun, "Recursive tracking of vascular networks in angiograms based on the detection-deletion scheme", IEEE Transaction on Medical Imaging, Vol. 12, No. 2, pp. 334–341, 1993.
[6] Y. A. Tolias, S. M. Panas, "A fuzzy vessel tracking algorithm for retinal images based on fuzzy clustering", IEEE Transaction on Medical Imaging, Vol. 17, No. 4, pp. 263–273, 1998.
[7] A. Can, H. Shen, J. N. Turner, H. L. Tanenbaum, B. Roysam, "Rapid automated tracing and feature extraction from retinal fundus images using direct exploratory algorithms", IEEE Transaction on Information Technology in Biomedicine, Vol. 3, No. 2, pp. 125–138, 1999.
[8] X. Jiang, D. Mojon, "Adaptive local thresholding by verification based multithreshold probing with application to vessel detection in retinal images", IEEE Transaction on Pattern Analysis and Machine Intelligence, Vol. 25, No. 1, pp. 131–137, 2003.
[9] F. Zana, J. Klein, "Segmentation of vessel-like patterns using mathematical morphology and curvature evaluation", IEEE Transaction on Image Processing, Vol. 10, No. 7, pp. 1010–1019, 2001.
[10] S. Chaudhuri, S. Chatterjee, N. Katz, M. Nelson, M. Goldbaum, "Detection of blood vessels in retinal images using two dimensional matched filters", IEEE Transaction on Medical Imaging, Vol. 8, No. 3, pp. 263–269, 1989.
[11] M. Al-Rawi, M. Qutaishat, M. Arrar, "An improved matched filter for blood vessel detection of digital retinal images", Computers in Biology and Medicine, Vol. 37, pp. 262–267, 2007.
[12] F. Zana, J.C. Klein, "Segmentation of vessel like patterns using mathematical morphology and curvature evaluation", IEEE Transaction on Image Processing, Vol. 10, No. 7, pp. 1010–1019, 2001.
[13] J.J. Staal, M.D. Abramoff, M. Niemeijer, M.A. Viegever, B. van Ginneken, "Ridge based vessel segmentation in color images of the retina", IEEE Transaction on Medical Imaging, Vol. 23, No. 4, pp. 501–509, 2004.
[14] R. Kirsch, "Computer determination of the constitute structure of biomedical images", Computers in Biomedical Research, Vol. 4, No. 3, pp. 315–328, 1971.

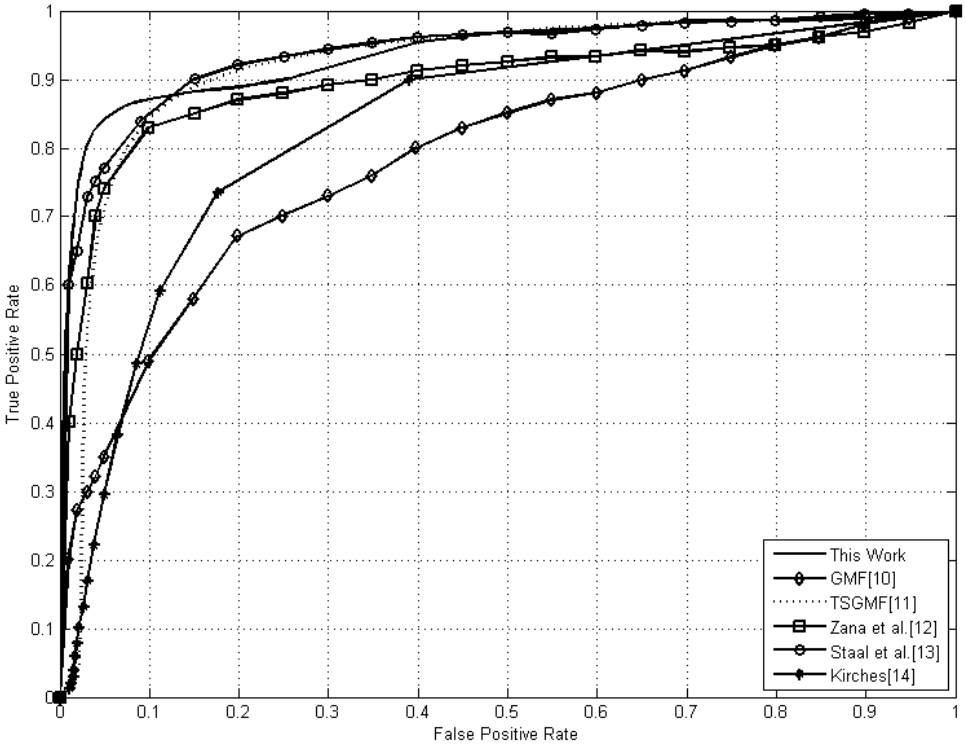

Fig. 9. Comparison of ROC curves